Statistical mechanics of wind wave-induced erosion in shallow tidal basins: Inferences from the Venice Lagoon

Andrea D'Alpaos,[1] Luca Carniello,[2] and Andrea Rinaldo[2,3]

Received 13 May 2013; revised 12 June 2013; accepted 14 June 2013.

[1] Wind wave-induced erosional effects are among the chief landscape-forming processes in tidal biomorphodynamics. Wave-driven bottom erosion, in fact, controls the equilibrium elevation and dynamics of subtidal and tidal flat surfaces, and the impact of waves against salt marsh margins influences their stability. The relevance of predictive studies projecting wind wave patterns in space and time is thus notable especially in view of the limited insight gained so far. Here we have employed a complete, coupled finite element model accounting for the role of wind waves and tidal currents on the hydrodynamic circulation in shallow basins to analyze the characteristics of combined current- and wave-induced exceedances in bottom shear stress over a given threshold for erosion. The results of our analyses from the Venice Lagoon suggest that wind wave-induced resuspension events can be modeled as a marked Poisson process, thus allowing one to set up a theoretical framework which can be used to model wind wave effects through the use of Monte Carlo realizations. This bears important consequences for quantitative analyses of the long-term biomorphodynamic evolution of tidal landscapes. **Citation:** D'Alpaos, A., L. Carniello, and A. Rinaldo (2013), Statistical mechanics of wind wave-induced erosion in shallow tidal basins: Inferences from the Venice Lagoon, *Geophys. Res. Lett.*, *40*, doi:10.1002/grl.50666.

1. Introduction

[2] Wind waves and related erosion processes play a critical role in the biomorphodynamic evolution of tidal landscapes. Sediment deposition, wave-induced erosion, and the rate of relative sea level rise determine the equilibrium elevation and dynamics of subtidal platforms and tidal flats [e.g., *Allen and Duffy*, 1998; *Fagherazzi et al.*, 2006; *Green and Coco*, 2007; *Marani et al.*, 2010; *D'Alpaos et al.*, 2012]. Moreover, the balance between horizontal progradation of salt marshes and wind wave erosion of their boundaries dictates the position of the marsh edge [e.g., *Möller et al.*, 1999; *Mariotti and Fagherazzi*, 2010; *Marani et al.*, 2011]. Both in the vertical and in the horizontal planes, temporal and spatial patterns of wind wave bottom shear stresses (BSSs) have important implications on the morphological and biological features of the tidal landscape [e.g., *Carniello et al.*, 2005; *Fagherazzi and Wiberg*, 2009; *Mariotti et al.*, 2010]. Intense wave-induced BSSs may lead to the disruption of the polymeric microphytobenthic biofilm [e.g., *Amos et al.*, 2004] and promote the resuspension of sediments transported within the basin by tidal currents, thus influencing light availability in the water column [e.g., *Lawson et al.*, 2007] and consequently the stability of sea grass ecosystems [e.g., *Carr et al.*, 2010]. Finally, because of their effect on the equilibrium elevation of tidal flats [e.g., *Marani et al.*, 2010], wave-induced erosion processes contribute to controlling the size of the tidal prism and related morphological features of tidal networks, such as channel cross-sectional areas [e.g., *D'Alpaos et al.*, 2010] and drainage density [e.g., *Marani et al.*, 2003; *Stefanon et al.*, 2012].

[3] Numerical models provide ways to describe hydrodynamic and wind wave fields in shallow tidal basins [e.g., *Umgiesser et al.*, 2004; *Carniello et al.*, 2005] and their influence on the morphodynamic evolution of tidal landscapes. Modeling tidal landscape morphodynamic evolution over timescales of centuries, however, calls for the use of simplified approaches [e.g., *Murray*, 2007] due to the numerical burdens involved when using full-fledged models, thus justifying analyses of the type proposed herein. Our aim is to develop a synthetic theoretical framework to represent wind wave-induced resuspension events and account for their erosional effects on the long-term biomorphodynamic evolution of tidal systems. To this end, we have applied a fully coupled wind wave-tidal model (WWTM) [*Carniello et al.*, 2005, 2011] to the Venice Lagoon, the largest Mediterranean brackish water body characterized by an average tidal range of about 1 m, with maximum tidal excursions of ± 0.75 m around mean sea level (msl). Our key result, emerging from the analysis of the local, temporal evolution of the modeled BSSs, is that wave-induced resuspensions can be seen as marked Poisson processes, in analogy with the occurrence of precipitation [e.g., *Rodriguez-Iturbe et al.*, 1987, 1988], shallow landslides [e.g., *D'Odorico and Fagherazzi*, 2003], and fires [e.g., *D'Odorico et al.*, 2006], or with processes obtained censoring Poisson rainfall arrivals via a soil moisture dynamics [e.g., *Botter et al.*, 2007]. A proper statistical mechanics, possibly applied in a predictive manner generating Monte Carlo realizations of long-term evolution of tidal water bodies, is therefore in sight for the biomorphodynamic evolution of tidal landscapes.

2. Methods

[4] The WWTM employed herein describes, on the same computational grid, the hydrodynamic flow field together with the generation and propagation of wind waves (see the

Additional supporting information may be found in the online version of this article.

[1]Department of Geosciences, University of Padova, Padua, Italy.
[2]Department of Civil, Environmental and Architectural Engineering (ICEA), University of Padova, Padua, Italy.
[3]Laboratory of Ecohydrology (ECHO), IEE, ENAC, École Polytechnique Fédérale de Lausanne, Lausanne, Switzerland.

Corresponding author: A. D'Alpaos, Department of Geosciences, University of Padua, Padua, Italy. (andrea.dalpaos@unipd.it)

0094-8276/13/10.1002/grl.50666

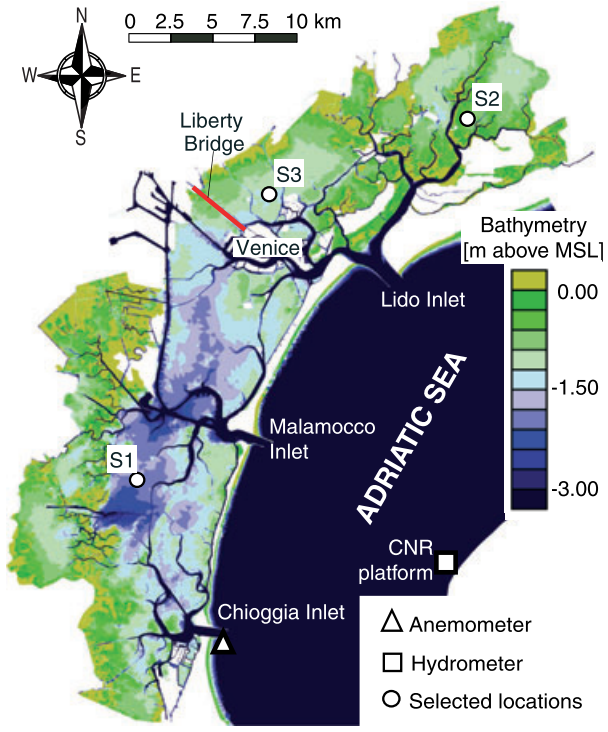

Figure 1. The Venice Lagoon has an area of about 550 km^2, is about 50 km long and 10 km wide, and is characterized by a semidiurnal tidal regime with a tidal range of about 1 m. The lagoonal bottom is mainly composed of cohesive sediments (representative D_{50} = 20 μm), a part form the main channels branching from the three inlets where sediments are coarser (mainly sand, with representative D_{50} = 200 μm). The image shows a color-coded bathymetry of the Venice Lagoon associated to the computational grid used in our simulations, which was constructed on the basis of the most recent (2003) and accurate bathymetric data (see the supporting information for details). The locations of the anemometric (Chioggia) and mareographic (CNR Oceanographic Platform) stations are shown, together with the locations of three stations for which we provide detailed characteristics of wave-induced resuspension events (see Figures 2 and 3).

supporting information and *Carniello et al.* [2005, 2011] for a detailed description of the model). The hydrodynamic model solves the 2-D shallow water equations using a semi-implicit staggered finite element method based on Galerkin's approach [*D'Alpaos and Defina*, 2007], thus yielding water levels which are used by the wind wave model to assess wave group celerity and bottom influence on wave propagation. The wind wave model is based on the solution of the wave action conservation equation, parameterized using the zero-order moment of the wave action spectrum in the frequency domain [*Carniello et al.*, 2005, 2011]. The model can also account for the spatial variability of the wind forcing, through an interpolation procedure of the available wind data [e.g., *Brocchini et al.*, 1995; *Carniello et al.*, 2012]. The WWTM has been largely tested against field observations in the Venice Lagoon and the Virginia Coast Reserve lagoons [e.g., *D'Alpaos and Defina*, 2007; *Carniello et al.*, 2011; *Mariotti et al.*, 2010], thus suggesting that the model is suited to computing temporal and spatial variations of the BSS in shallow microtidal basins. Numerical simulations were carried out on a computational grid which represents the Venice Lagoon and a portion of the Adriatic Sea (see Figure 1) and consists of about 52,000 nodes and about 100,000 triangular elements. The model was forced by using hourly tidal levels measured at the Consiglio Nazionale delle Ricerche (CNR) Oceanographic Platform, located in the Adriatic Sea in front of the Venice Lagoon (see Figure 1), and wind velocities and directions observed at the Chioggia anemometric station, for which various 1 year long time series of wind data were available. We forced the model with the time series recorded in 2005, which was shown to be a "representative" year for the wind characteristics in the Venice Lagoon. The probability distribution of wind velocities for the time series recorded in 2005 was, in fact, the closest to the mean of the probability distributions computed for every year between 2000 and 2008.

[5] At any location within the Venice Lagoon, we analyzed the temporal evolution of the BSS on the basis of a "Peaks Over Threshold" (POT) method, once a critical shear stress for erosion was chosen [*Amos et al.*, 2004]. Finally, we verified whether or not wind wave resuspension events could be modeled as a Poisson process; i.e., we performed a Kolmogorov-Smirnov (KS) goodness of fit test to test the hypothesis that the interarrival time of resuspension events (the time between two consecutive resuspension occurrences) is an exponentially distributed random variable.

3. Results and Discussion

[6] We first start by considering three locations (*S*1, *S*2, and *S*3) in the Venice Lagoon for which we provide a detailed description of model results (see Figure 2 for station *S*3) and the statistical characteristics of wave-induced resuspension events (see Figure 3 for all stations). The three stations (see Figure 1) were selected to represent three different typical environments in the Venice Lagoon: (i) a subtidal platform (depth of 2.0 m below msl) in the deepest part of the lagoon, fetch unlimited to the most frequent and intense wind directions of Bora (blowing from NE) and Scirocco (blowing from SE) (*S*1); (ii) a very shallow tidal flat (depth of 0.75 m) located in the northern part of the lagoon where large salt marsh areas are present (*S*2); and (iii) a tidal flat (depth of 1.10 m) in the area between the city of Venice and the Marco Polo Airport (*S*3). Fluctuating tidal levels (Figure 2b) and the related tidal current velocities control the temporal evolution of current-induced BSSs, τ_{tc} (Figure 2c), which however are not strong enough to produce bottom erosion on the unchanneled portions of the tidal basin. Current-induced BSSs, in fact, are well below the critical shear stress for erosion, τ_c = 0.4 Pa [e.g., *Amos et al.*, 2004; *Marani et al.*, 2010; *Mariotti et al.*, 2010], displayed by the continuous red lines in Figures 2c–2e. Wind intensities, together with local fetch and water depths, govern the temporal evolution of wave-induced BSSs, τ_{ww} (Figure 2d), whereas it is worth noting that the total BSS, τ_{cw}, determined by the combined action of currents and waves (Figure 2e), is enhanced beyond the sum of the two contributions [e.g., *Soulsby*, 1995]. Figure 2f shows the effect of the nonlinear interaction between waves and currents by portraying the temporal evolution of the difference $\tau_{cw} - (\tau_{tc} + \tau_{ww})$

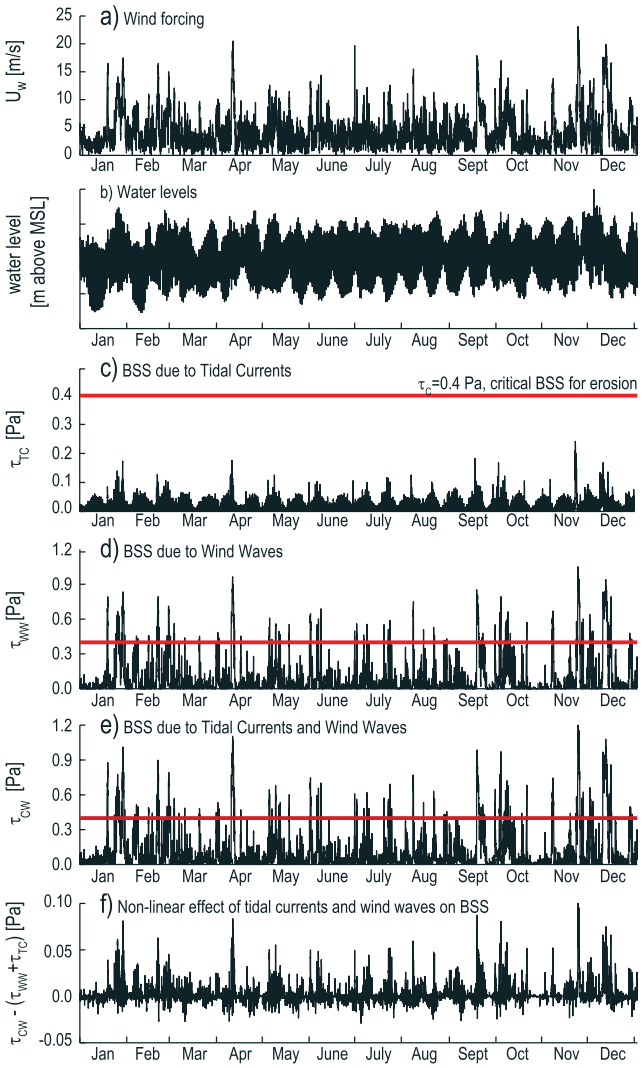

Figure 2. Wind forcings and model results at the S3 station (see Figure 1). Time series of (a) the forcing wind speeds measured in 2005; (b) computed water levels; (c) BSS produced by tidal currents, τ_{tc}; (d) BSS produced by wind waves, τ_{ww}; (e) BSS resulting from the combined effect of tidal currents and wind waves, τ_{cw}; and (f) effect of the nonlinear interaction between waves and currents, $\tau_{cw} - (\tau_{ww} + \tau_{tc})$. The red lines indicate the threshold BSS for erosion, τ_c = 0.4 Pa.

which can be as large as 10% of the total BSS. Although wave-induced BSSs are larger than those induced by tidal currents, the latter play a significant role in modulating the temporal evolution of the total BSS, furthermore increasing peak BSS values by up to 30%, as also observed by *Mariotti et al.* [2010], thus importantly affecting the occurrence of overthreshold exceedances.

[7] In order to provide a statistical characterization of wave-induced resuspension events, we have analyzed the time series of computed total BSSs, τ_{cw}, on the basis of a POT method. This allowed us to identify times of cross-up and cross-down of BSS with respect to the critical value (and therefore single resuspension events), the interarrival times of resuspension events (the time between two consecutive cross-ups), their maximum intensity (the peak excess, defined as the largest excess in a cluster of overthreshold BSSs, $(\tau_{cw} - \tau_c)_{max}$), and duration (time between a cross-up and the following cross-down, during which the BSS stays over the threshold). The time series of BSSs were preliminarily low-pass filtered through a moving average operation (with a 6 h span) in order to remove short-term fluctuations, leading to spurious upcrossing and downcrossing of the fixed threshold, without losing the modulation given by the semidiurnal tidal oscillation. Such a procedure is necessary to meet the assumptions embedded in our analysis which require resuspension events to be independent (see the supporting information for further details). Figure 3 compares the computed exceedance probabilities (circles) of interarrival times (Figures 3a–3c), maximum intensities of overthreshold events (Figures 3d–3f), and durations of

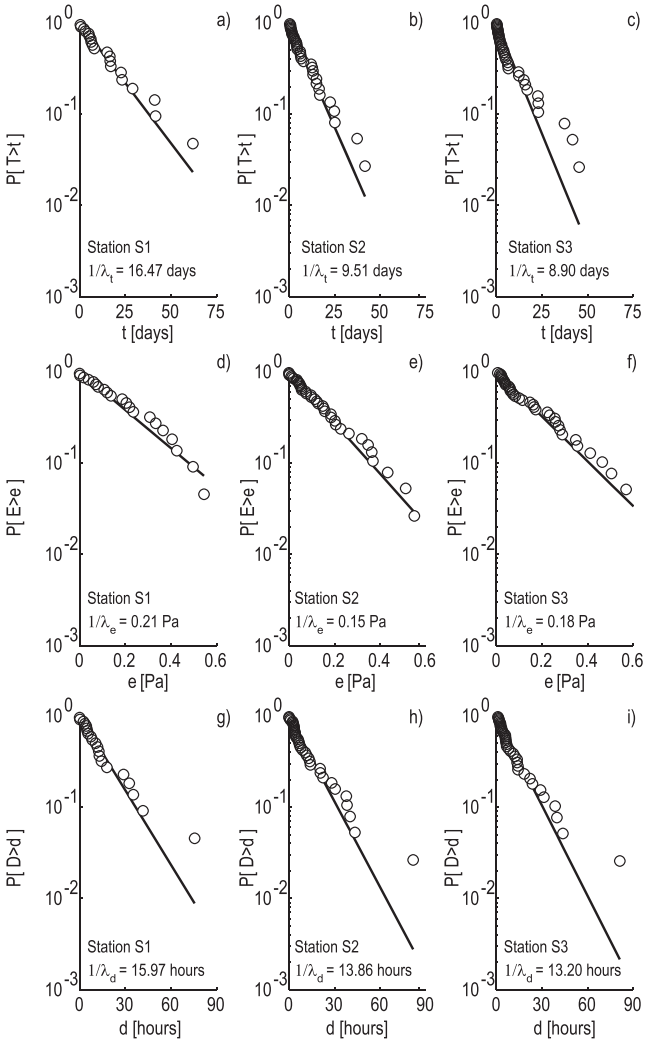

Figure 3. Statistical characterization of resuspension events at three stations (S1, S2, and S3) within the lagoon (see Figure 1). Probability distributions of (a–c) interarrival times, t; (d–f) intensities of peak excesses in the BSS over a critical threshold (i.e., maximum intensities of the exceedances during an event, $e = (\tau_{tc} - \tau_c)_{max}$); and (g–i) durations of overthreshold events. The circles represent the computed probability distributions, while the solid lines represent the theoretical exponential trend.

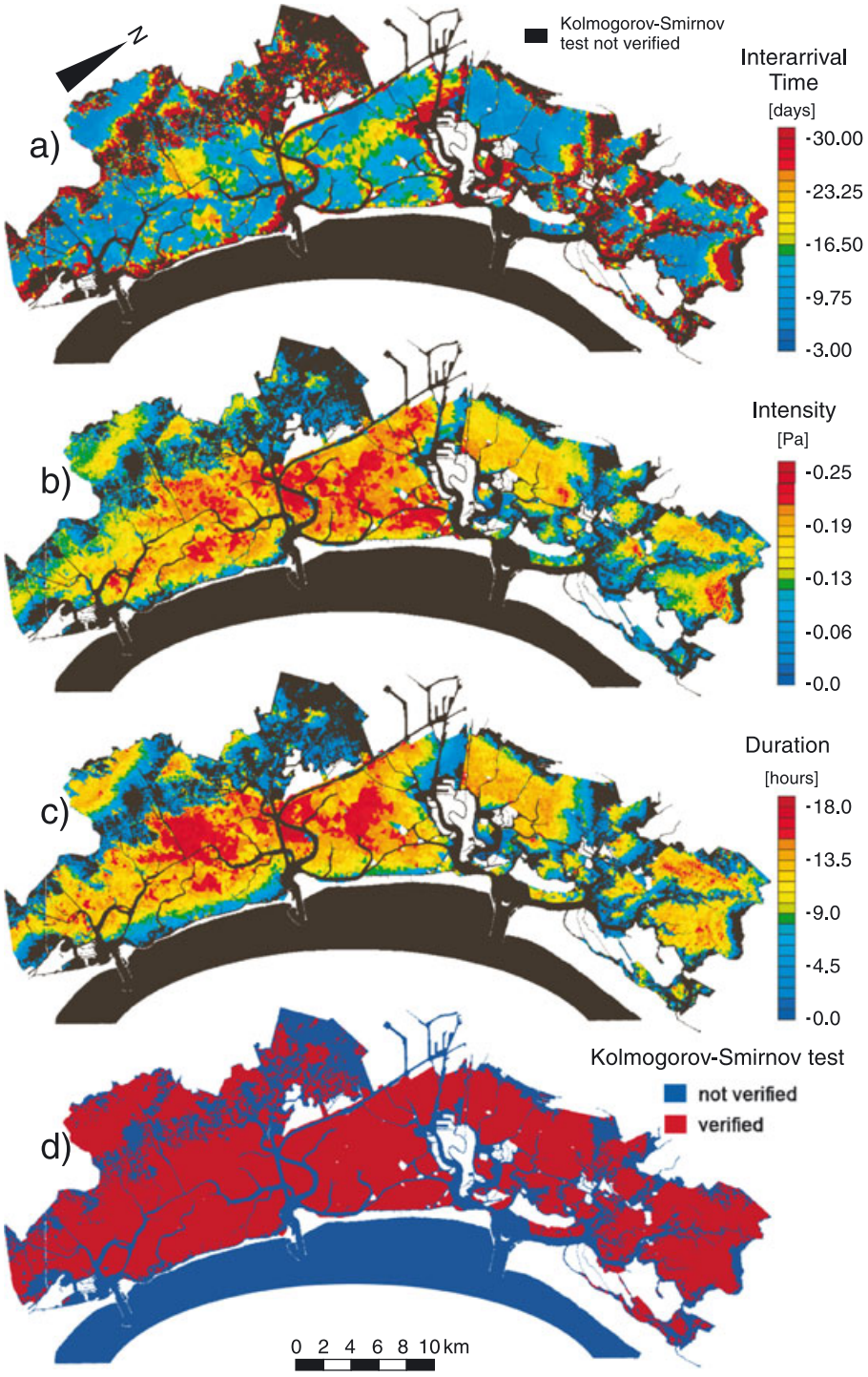

Figure 4. Spatial distributions of (a) mean interarrival times, (b) mean intensities of peak excesses, and (c) mean durations of overthreshold exceedances, at sites where wind resuspension events can be modeled as a marked Poisson process; (d) sites where the probability distributions of local interarrival times, intensities of peak excesses, and durations of overthreshold events are exponential, as confirmed by the KS test ($\alpha = 0.05$).

overthreshold events (Figures 3g–3i) with the theoretical exponential trend (solid lines), for the three selected locations (*S*1, *S*2, and *S*3).

[8] We first note that the interarrival time of resuspension events is described by an exponential distribution (Figures 3a–3c). The parameter λ_t of the exponential distribution is the mean rate of occurrence of wave-induced resuspension events; i.e., $1/\lambda_t$ is their mean interarrival time. This observation is quantitatively supported by the results of the KS test which is satisfied in all the cases (sites *S*1, *S*2, and *S*3) at significance level $\alpha = 0.05$. We also note that both the peak excess $(\tau_{cw} - \tau_c)_{max}$ and the duration of the resuspension events reveal to be exponentially distributed random variables, with mean $1/\lambda_e$ and $1/\lambda_d$, respectively (Figures 3d–3f

and 3g–3i, respectively). The KS test performed for those probability distributions is satisfied in all the cases, at significance level $\alpha = 0.05$. The mean interarrival times for the three considered locations range between about 9 and 16 days, whereas the mean durations range between 13 and 16 h, and the mean peak excesses characterizing the resuspension events range between 0.15 and 0.21 Pa. The parameters of the exponential distributions display some spatial variability as we show in Figure 4.

[9] Before analyzing the spatial variability of mean interarrival times, peak excesses, and durations, it is worthwhile recalling that the shear stress induced on the bottom by wind waves generally depends on wind velocity, fetch, and water depth. For any prescribed wind intensity and fetch, the relationship between BSS and water depth is represented by a curve peaking at some intermediate water depths: For both small and large depths, wind waves do not induce appreciable BSSs. As wind velocity increases (for a fixed fetch), the BSS increases and peaks at progressively lower water depths; as fetch increases (for a fixed velocity), the BSS increases and peaks at progressively larger water depths [e.g., *Fagherazzi et al.*, 2006; *Marani et al.*, 2010]. Water depth is a function of basin bathymetry and local tidal levels, whereas fetch depends on basin morphology (for the sheltering effect of, e.g., salt marshes on adjacent downwind flats) and water depth. The observations above suggest that the characteristics of resuspension events display complex spatial patterns, as it emerges from Figure 4 which portrays the mean interarrival time (Figure 4a), peak excess (Figure 4b), and duration of overthreshold events (Figure 4c) at any location within the Venice Lagoon in which the KS test, made in order to verify that the mentioned variables are exponentially distributed random variables, is satisfied at significance level $\alpha = 0.05$ (Figure 4d).

[10] Interestingly, we note that portions of the lagoon in which wind wave-induced resuspension events cannot be modeled as a Poisson process are mostly represented by salt marshes and tidal channel networks (Figure 4d). No exceedances over the fixed threshold, τ_c, tend to occur over salt marsh platforms because of the reduced water depth [e.g., *Carniello et al.*, 2005; *Möller et al.*, 1999]. Within the channel network, exceedances do tend to occur but these are mostly related to peak excesses promoted by tidal currents, which cannot be modeled as a Poisson process (Figure 4d). Large interarrival times (Figure 4a) are found leeward of spits, marsh platforms, islands, or artificial structures (see, e.g., the Liberty Bridge in Figure 1) which provide a sheltering effect particularly to Bora wind, the most intense and morphologically significant wind in the Venice Lagoon. This occurs, in particular, at sites sheltered by marshes and the mainland in the northeastern part of the Venice Lagoon and in its western portions (see Figure 1). On the contrary, short interarrival times characterize fetch-unlimited portions of the lagoon with depths around 1.5 m below msl at which wave-induced BSSs are known to reach their maximum intensity [e.g., *Fagherazzi et al.*, 2006; *Carniello et al.*, 2009]. Portions of the lagoon much deeper or much shallower than 1.5 m below msl, or characterized by smaller fetch, display intermediate interarrival times (Figure 4a).

[11] Overthreshold peak intensities (Figure 4b) and durations (Figure 4c) are much larger in the central and southern parts of the Venice Lagoon, than in its northern part, which is sheltered by the mainland from Bora winds and is characterized by the presence of very shallow flats and large salt marsh portions which also provide sheltering effects. Overthreshold peak intensities and durations display their maximum values in the fetch-unlimited central portions of the lagoon characterized by water depths around 1.5 m. Large overthreshold peak intensities and long durations are also found to occur in the southern part of the lagoon. This agrees with recent observations emphasizing a critical erosive trend for the tidal flats and subtidal platforms in the central-southern part of the Venice Lagoon, where fine sediments are eroded from the bottom during intense storm events and transported toward the inlets where they are flushed out of the lagoon [e.g., *Amos et al.*, 2004; *Carniello et al.*, 2009; *D'Alpaos*, 2010].

[12] Finally, we observe that if detailed bed compositions were known over the domain, together with the spatial distribution of sea grasses, microphytobenthos, and halophytic vegetation, the proposed framework would allow one to account for related spatial variabilities in the threshold shear stress. We also recall that the POT formulation of the extreme value theory prescribes that for increasing censoring thresholds, the exceedances must be Poisson distributed [*Cramer and Leadbetter*, 1967]. As the threshold increases, the process is therefore known to remain Poisson, but obviously, longer and longer simulations are required in order to contrive meaningful statistics, owing to the progressively rarer events producing a BSS larger than τ_c. This is true as long as the threshold can still be exceeded. In the case of decreasing thresholds, the process remains Poisson provided that the threshold is high enough to exclude "deterministic" exceedances, such as those related to tidal currents, in our case (see the supporting information for detailed discussion on the effects of different threshold values).

[13] We believe that our analyses may help refine our understanding of the effect of wave-driven erosion processes on the biomorphodynamic evolution of the tidal landscape, demonstrating, in particular, that these processes can be described as marked Poisson processes with exponentially distributed interarrival times, intensities, and durations. We speculate that the importance of our approach for long-term biomorphodynamic studies lies in the technical possibility put forward to generate Poissonian sequences of forcings through which Monte Carlo realizations of relevant morphological evolutions can be computed. Ensemble averages of possible realizations will thus allow significantly accurate predictions of long-term morphologies and their expected uncertainty.

[14] **Acknowledgments.** This work was supported by the CARIPARO Project titled "Reading signatures of the past to predict the future: 1000 years of stratigraphic record as a key for the future of the Venice Lagoon." A.D. thanks "Thetis spa" for financial support, L.C. thanks "Fondazione Vajont" for financial support. The authors thank two anonymous reviewers for their comments.

[15] The Editor thanks two anonymous reviewers for their assistance in evaluating this paper.

References

Allen, J. R. L., and M. J. Duffy (1998), Medium-term sedimentation on high intertidal mudflats and salt marshes in the Severn Estuary, SW Britain: The role of wind and tide, *Mar. Geol.*, *150*(1-4), 1–27.

Amos, C. L., A. Bergamasco, G. Umgiesser, S. Cappucci, D. Cloutier, L. DeNat, M. Flindt, M. Bonardi, and S. Cristante (2004), The stability of tidal flats in Venice Lagoon—The results of in-situ measurements using two benthic, annular flumes, *J. Mar. Syst.*, *51*, 211–241.

Botter, G., A. Porporato, I. Rodriguez-Iturbe, and A. Rinaldo (2007), Basin-scale soil moisture dynamics and the probabilistic characterization of carrier hydrologic flows: Slow, leaching-prone components of the hydrologic response, *Water Resour. Res.*, *43*, W02417, doi:10.1029/2006WR005043.

Brocchini, M., M. G. Wurtele, G. Umgiesser, and S. Zecchetto (1995), Calculation of a mass-consistent two-dimensional wind field with divergence control, *J. Appl. Meteorol.*, *34*(11), 2543–2555.

Carniello, L., A. Defina, S. Fagherazzi, and L. D'Alpaos (2005), A combined wind wave-tidal model for the Venice Lagoon, *J. Geophys. Res.*, *110*, F04007, doi:10.1029/2004JF000232.

Carniello, L., A. Defina, and L. D'Alpaos (2009), Morphological evolution of the Venice Lagoon: Evidence from the past and trend for the future, *J. Geophys. Res.*, *114*, F04002, doi:10.1029/2008JF001157.

Carniello, L., A. D'Alpaos, and A. Defina (2011), Modeling wind waves and tidal flows in shallow micro-tidal basins, *Estuarine Coastal Shelf Sci.*, *92*, 263–276, doi:10.1016/j.ecss.2011.01.001.

Carniello, L., A. Defina, and L. D'Alpaos (2012), Modeling sand-mud transport induced by tidal currents and wind waves in shallow microtidal basins: Application to the Venice Lagoon (Italy), *Estuarine Coastal Shelf Sci.*, *102*, 105–115, doi:10.1016/j.ecss.2012.03.016.

Carr, J., P. D'Odorico, K. McGlathery, and P. Wiberg (2010), Stability and bistability of seagrass ecosystems in shallow coastal lagoons: Role of feedbacks with sediment resuspension and light attenuation, *J. Geophys. Res.*, *115*, G03011, doi:10.1029/2009JG001103.

Cramer, H., and M. R. Leadbetter (1967), *Stationary and Related Stochastic Processes*, 348 pp., John Wiley, New York.

D'Alpaos, L. (2010), *Fatti e misfatti di idraulica lagunare*, Ist. Veneto di Sci. Lett. e Arti, Venice, Italy.

D'Alpaos, L., and A. Defina (2007), Mathematical modeling of tidal hydrodynamics in shallow lagoons: A review of open issues and applications to the Venice Lagoon, *Comput. Geosci.*, *33*, 476–496, doi:10.1016/j.cageo.2006.07.009.

D'Alpaos, A., S. Lanzoni, M. Marani, and A. Rinaldo (2010), On the tidal prism-channel area relations, *J. Geophys. Res.*, *115*, F01003, doi:10.1029/2008JF001243.

D'Alpaos, A., C. Da Lio, and M. Marani (2012), Biogeomorphology of tidal landforms: Physical and biological processes shaping the tidal landscape, *Ecohydrology*, *5*, 550–562, doi:10.1002/eco.279.

D'Odorico, P., and S. Fagherazzi (2003), A probabilistic model of rainfall-triggered shallow landslides in hollows: A long-term analysis, *Water Resour. Res.*, *39*(9), 1262, doi:10.1029/2002WR001595.

D'Odorico, P., F. Laio, and L. Ridolfi (2006), A probabilistic analysis of fire-induced tree-grass coexistence in savannas, *Am. Nat.*, *167*(3), E79–E87.

Fagherazzi, S., L. Carniello, L. D'Alpaos, and A. Defina (2006), Critical bifurcation of shallow microtidal landforms in tidal flats and salt marshes, *Proc. Natl. Acad. Sci. U.S.A.*, *103*(22), 8337–8341, doi:10.1073/pnas.0508379103.

Fagherazzi, S., and P. L. Wiberg (2009), Importance of wind conditions, fetch, and water levels on wave-generated shear stresses in shallow intertidal basins, *J. Geophys. Res.*, *114*, F03022, doi:10.1029/2008JF001139.

Green, M. O., and G. Coco (2007), Sediment transport on an estuarine intertidal flat: Measurements and conceptual model of waves, rainfall and exchanges with a tidal creek, *Estuarine Coastal Shelf Sci.*, *72*, 553–569, doi:10.1016/j.ecss.2006.11.006.

Lawson, S. E., P. L. Wiberg, K. J. McGlathery, and D. C. Fugate (2007), Wind-driven sediment suspension controls light availability in a shallow coastal lagoon, *Estuaries Coasts*, *30*(1), 102–112.

Marani, M., E. Belluco, A. D'Alpaos, A. Defina, S. Lanzoni, and A. Rinaldo (2003), On the drainage density of tidal networks, *Water Resour. Res.*, *39*(2), 105–113.

Marani, M., A. D'Alpaos, S. Lanzoni, L. Carniello, and A. Rinaldo (2010), The importance of being coupled: Stable states and catastrophic shifts in tidal biomorphodynamics, *J. Geophys. Res.*, *115*, F04004, doi:10.1029/2009JF001600.

Marani, M., A. D'Alpaos, S. Lanzoni, and M. Santalucia (2011), Understanding and predicting wave erosion of marsh edges, *Geophys. Res. Lett.*, *38*, L21401, doi:10.1029/2011GL048995.

Mariotti, G., and S. Fagherazzi (2010), A numerical model for the coupled long-term evolution of salt marshes and tidal flats, *J. Geophys. Res.*, *115*, F01004, doi:10.1029/2009JF001326.

Mariotti, G., S. Fagherazzi, P. L. Wiberg, K. J. McGlathery, L. Carniello, and A. Defina (2010), Influence of storm surges and sea level on shallow tidal basin erosive processes, *J. Geophys. Res.*, *115*, C11012, doi:10.1029/2009JC005892.

Möller, I., T. Spencer, J. R. French, D. J. Leggett, and M. Dixon (1999), Wave transformation over salt marshes: A field and numerical modelling study from North Norfolk, England, *Estuarine Coastal Shelf Sci.*, *49*(3), 411–426, doi:10.1006/ecss.1999.0509.

Murray, A. B. (2007), Reducing model complexity for explanation and prediction, *Geomorphology*, *90*(3-4), 178–191, doi:10.1016/j.geomorph.2006.10.020.

Rodriguez-Iturbe, I., D. R. Cox, and V. Isham (1987), Some models for rainfall based on stochastic point processes, *Proc. R. Soc. London, Ser. A*, *410*, 269–288.

Rodriguez-Iturbe, I., D. R. Cox, and V. Isham (1988), A point process model for rainfall: Further developments, *Proc. R. Soc. London, Ser. A*, *410*, 283–298.

Soulsby, R. L. (1995), Bed shear-stresses due to combined waves and currents, in *Advances in Coastal Morphodynamics*, edited by Stive, M. J. F. et al., pp. 4-20–4-23, Delft Hydraul., Delft, Netherlands.

Stefanon, L., L. Carniello, A. D'Alpaos, and A. Rinaldo (2012), Signatures of sea level changes on tidal geomorphology: Experiments on network incision and retreat, *Geophys. Res. Lett.*, *39*, L12402, doi:10.1029/2012GL051953.

Umgiesser, G., M. Sclavo, S. Carniel, and A. Bergamasco (2004), Exploring the bottom stress variability in the Venice Lagoon, *J. Mar. Syst.*, *51*, 161–178.